

ELECTRONIC SUPPLEMENTARY INFORMATION

Ion and radical chemistry in $(\text{H}_2\text{O}_2)_N$ clusters

Andriy Pysanenko, Eva Pluhařová, Ivo S. Vinklárek,^a Jozef Rakovský, Viktoriya Poterya, Jaroslav Kočišek, and Michal Fárník*

J. Heyrovský Institute of Physical Chemistry, v.v.i., Czech Academy of Sciences; Dolejškova 2155/3, 182 23 Prague, Czech Republic. Fax: +420 28658 2307; Tel: +420 26605 3206
E-mail: *michal.farnik@jh-inst.cas.cz*

^aalso affiliated at: Faculty of Mathematics and Physics, Charles University, Ke Karlovu 3, 121 16 Prague 2, Czech Republic

1 Ionization thresholds

Figure 1 shows the electron energy dependent ion yield of different mass peaks in the positive mass spectra. All the yields were measured with the molecular beam present, however, some of them correspond to the diffused molecular background as confirmed by the background measurement. Left panel (a) summarizes the ion yields for individual molecules. Ar^+ ions can originate from Ar clusters or from Ar monomers in the beam. The threshold seems somewhat lower than the NIST value of Ar ionization energy of 15.76 eV, in accordance with the shift of the ionization energy in clusters due to solvation effects. The Ar_2^+ ion, which definitely originates from the clusters, exhibits threshold around 15 eV. However, the signal to noise ratio of this ion signal is much lower than for the Ar^+ ion in our present experiment. The water H_2O^+ ion yield from the background exhibits threshold in agreement with the water ionization energy 12.62 eV reported at NIST. The hydrogen peroxide H_2O_2^+ ion yield also corresponds to the diffused molecule background, and the observed threshold is in a rough agreement with the corresponding ionization energy of H_2O_2 molecule at 10.58 eV, although it might be somewhat higher in our measurements. The urea $\text{CH}_4\text{N}_2\text{O}^+$ (labeled as U^+) ion yield also corresponds to the diffused molecules and exhibits a threshold at the expected value of 10.3 eV. Thus, all the observed thresholds are in relatively good agreement with the literature values within the energy resolution of our experiment of approximately 0.5 eV, considering also the low signal to noise ratio of some ion yields.

In the right hand side panel (b), we summarize the ion yields of some ions which unambiguously originate from the clusters: $(\text{H}_2\text{O}_2)_7^+$, $(\text{H}_2\text{O}_2)_7\text{H}^+$, $(\text{H}_2\text{O}_2)_7\text{H}_3\text{O}^+$, $(\text{H}_2\text{O}_2)_7\text{H}_2\text{O}\cdot\text{H}_3\text{O}^+$, and $\text{U}\cdot(\text{H}_2\text{O}_2)_2\text{H}^+$. All these ion yields exhibit essentially the same threshold around 15 eV within our experimental error bars. It ought to be mentioned that also all other cluster ions exhibited the same thresholds. The reported NIST energies of dissociative ionization of hydrogen peroxide yielding OH^+ , H_2O^+ and HO_2^+ as well as O_2^+ fit the interval between 14.1 and 15.8 eV. Thus we are unable to resolve them within the present experiment. The observed cluster ions can be generated via the dissociative ionization of H_2O_2 . Alternatively, the observed threshold is consistent with the threshold observed for Ar ionization in the clusters, which indicates that the ionization mechanism

in the clusters could also proceed via the Ar ionization and subsequent charge transfer to the embedded molecular cluster. This model can be justified by the larger number of Ar atoms in the cluster compared to a few adsorbed molecules. The mean Ar_M size in the present case is $\bar{M} \approx 160$, and we have also repeated these experiments for much larger clusters with the same results. The mass spectra indicate that up to about 20 molecules could be adsorbed on Ar_M clusters, however, the large H_2O_2 cluster ions originated rather from the pickup on larger Ar_M clusters from the tail of the log-normal size distribution. Presumably, about ten molecules could be adsorbed on the mean size cluster with $\bar{M} \approx 160$ Ar atoms. Thus, the incoming electron most likely finds and ionizes Ar atom in the first place. However, the charge transfer to embedded molecular cluster seems to be very efficient, since we cannot see any strong Ar_n^+ fragment ions, already the dimer Ar_2^+ has a very weak signal. The results also point to very effective evaporation of Ar atoms from the cluster after the charge transfer process, since we cannot observe any mixed cluster ions with Ar even at the ionization electron energies close to the thresholds.

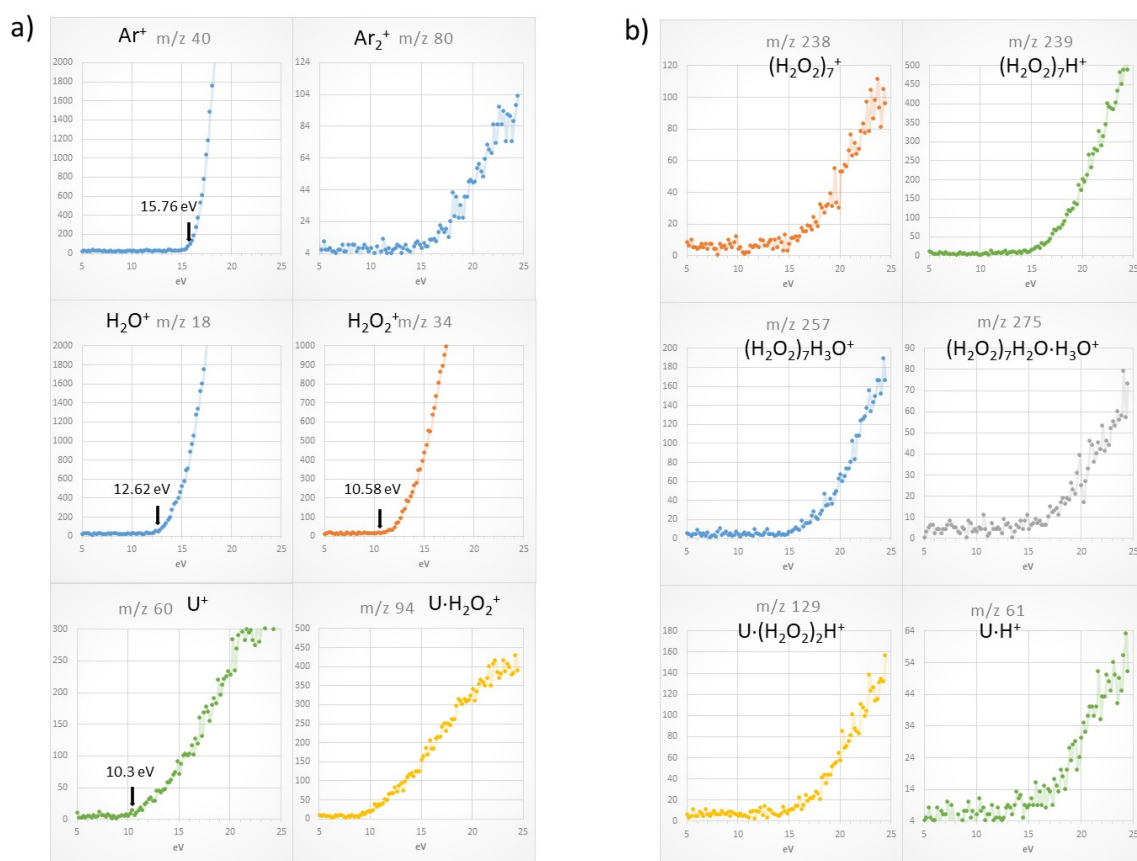


Figure 1. The electron energy dependent ion yield of different mass peaks in the positive mass spectra: (a) individual molecular ions (except for Ar_2^+ and possibly Ar^+); (b) cluster ions. The ions and their m/z are indicated. The vertical arrows indicate the gas phase molecule ionization energies from literature.

As the last remark, it is interesting to note that the last ion in panel (a), $\text{U}\cdot(\text{H}_2\text{O}_2)^+$, exhibits a low threshold consistent with urea molecule or even lower. Thus, the molecular complex $\text{U}\cdot(\text{H}_2\text{O}_2)$ is present in the background and is ionized as isolated complex, and the urea ionization energy might be lowered by the complexation with H_2O_2 .

2 Ion series

Figure 2 shows the dependence of the intensity of water-containing peaks in the mass spectra on the number of water molecules. Left panel shows the $(\text{H}_2\text{O}_2)_n(\text{H}_2\text{O})_k\text{H}^+$ series as a function of k . Four examples for $n = 1, 2, 3$ and 4 are shown. Further series with more H_2O_2 molecules exhibit the same dependencies. All the series follow essentially an exponential decay with the number of water molecules k with the exception of the single point $(\text{H}_2\text{O}_2)\text{H}^+$.

The right panel shows analogous series with O_2^- in the negative spectrum, $(\text{H}_2\text{O}_2)_n(\text{H}_2\text{O})_k\text{O}_2^-$. The strongest series for $n = 3, 4, 5$ and 7 are shown. Other series have essentially the same dependencies. Here the decay exhibits a step between $k = 1$ and 2 , i.e. the clusters with two water molecules are as abundant as the corresponding clusters with one H_2O , and in some cases the clusters with two water molecules are even more abundant. Assuming a pickup of some small H_2O impurity in the pickup cell, we would expect the intensities to decrease exponentially with the number of water molecules k , as is the case in the positive spectrum (left panel). The observed step-like behavior would invoke some special stability or preferential generation of the anion clusters with the water molecules $(\text{H}_2\text{O}_2)_n(\text{H}_2\text{O})_2\text{O}_2^-$. Since we have no argument supporting this hypothesis, we put forward an alternative assignment of the $(\text{H}_2\text{O}_2)_n(\text{H}_2\text{O})_k\text{O}_2^-$ series for $k = 1$ to $(\text{H}_2\text{O}_2)_{n+1}\text{O}_2^-$, and the series for $k = 2$ to $(\text{H}_2\text{O}_2)_{n+2}^-$, the series $k = 3$ to $(\text{H}_2\text{O}_2)_{n+2}\text{H}_2\text{O}^-$, and the series $k = 4$ to $(\text{H}_2\text{O}_2)_{n+2}(\text{H}_2\text{O})_2^-$.

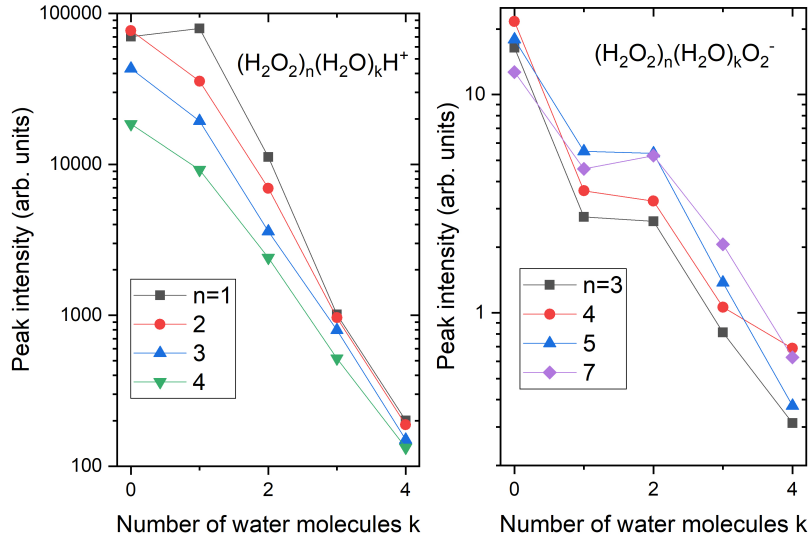


Figure 2. Intensities of mass peak series: $(\text{H}_2\text{O}_2)_n(\text{H}_2\text{O})_k\text{H}^+$ as a function of the number of water molecules k for $n = 1, 2, 3$ and 4 (left), and $(\text{H}_2\text{O}_2)_n(\text{H}_2\text{O})_k\text{O}_2^-$ series for $n = 3, 4, 5$ and 7 (right).

This alternative assignment assumes the transient negative ion (TNI) H_2O_2^- stabilization to yield $(\text{H}_2\text{O}_2)_n^-$, which has been observed in quite a few cases in clusters as discussed in the main article (e.g., $(\text{H}_2\text{O})_n^-$ is formed in electron attachment to water clusters while dissociative electron attachment (DEA) to water molecule yields OH^-). The generation of $(\text{H}_2\text{O}_2)_n\text{O}^-$ series could be also justified, since O^- ion is the product of the DEA to H_2O_2 molecule in the gas phase. The major product of DEA of H_2O_2 is the OH^- populated with 75% probability while O^- is populated with 25% probability. The series with one and two water molecules can either correspond to the H_2O_2^- or H_2O^- TNI stabilization, which is possible in clusters. Thus this assignment is fully plausible and

both possible assignments are discussed in the main article.

3 Positive ion reactions

Some of the positive ion cluster series discussed in the main manuscript can be generated in the $(\text{H}_2\text{O}_2)_N$ clusters via ion-molecule and radical reactions after the dissociative ionization of H_2O_2 , which can yield different ions. The possible reactions are summarized in the following Table 1. The heats of formation ΔH_f^0 , proton affinities PA , ionization energies IE , and appearance energies AE were taken from NIST Chemistry WebBook (<http://webbook.nist.gov>). Reaction enthalpies ΔH_r^0 were calculated and exothermic reactions ($\Delta H_r^0 \leq 0$) are listed.

Table 1. Possible ion-molecule and radical reactions in positively charged $(\text{H}_2\text{O}_2)_n^+$ clusters: heats of formation ΔH_f^0 , proton affinities PA , ionization energies IE , appearance energies AE , and reaction enthalpies ΔH_r^0 , all values in eV. Reactions corresponding to equations in the main manuscript are labeled. PT-proton transfer, CT-charge transfer.

Specie	ΔH_f^0	PA	IE
$\text{O}_2(^3\Sigma_g)$	0.00		12.07
H_2O	-2.51	7.16	12.62
H_2O_2	-1.41	6.99	10.58
O	2.58		
OH	0.40		13.02
HO_2	0.02		11.35
H	2.26		13.60
A) Dissociative ionization		AE	
$\text{H}_2\text{O}_2 + e^- \rightarrow \text{H}_2\text{O}^+ + \text{O} + 2e^-$	14.09		
$\text{H}_2\text{O}_2 + e^- \rightarrow \text{OH}^+ + \text{OH} + 2e^-$	15.35		
$\text{H}_2\text{O}_2 + e^- \rightarrow \text{HO}_2^+ + \text{H} + 2e^-$	15.36		
$\text{H}_2\text{O}_2 + e^- \rightarrow \text{O}_2^+ + \text{H}_2 + 2e^-$	15.8		
B) Radical reactions		ΔH_r^0	
$\text{O} + \text{H}_2\text{O}_2 \rightarrow \text{HO}_2 + \text{OH}$	-0.75		
$\text{HO}_2 + \text{OH} \rightarrow \text{H}_2\text{O} + \text{O}_2$	-2.93		
$\text{OH} + \text{H}_2\text{O}_2 \rightarrow \text{HO}_2 + \text{H}_2\text{O}$	-1.48	(Ia)	
$\text{H} + \text{H}_2\text{O}_2 \rightarrow \text{H}_2\text{O} + \text{OH}$	-2.96		
C) Cationic reactions		ΔH_r^0	
$\text{H}_2\text{O}_2^+ + \text{H}_2\text{O}_2 \rightarrow (\text{H}_2\text{O}_2)\text{H}^+ + \text{HO}_2$	-0.28	(1)	PT
$\text{H}_2\text{O}^+ + \text{H}_2\text{O}_2 \rightarrow \text{H}_2\text{O} + \text{H}_2\text{O}_2^+$	-2.04		CT
$\text{H}_2\text{O}^+ + \text{H}_2\text{O}_2 \rightarrow \text{OH} + (\text{H}_2\text{O}_2)\text{H}^+$	-0.84		PT
$\text{OH}^+ + \text{H}_2\text{O}_2 \rightarrow \text{OH} + \text{H}_2\text{O}_2^+$	-2.44		CT
$\text{OH}^+ + \text{H}_2\text{O}_2 \rightarrow \text{O} + (\text{H}_2\text{O}_2)\text{H}^+$	-1.97		PT
$\text{HO}_2^+ + \text{H}_2\text{O}_2 \rightarrow \text{HO}_2 + \text{H}_2\text{O}_2^+$	-0.77		CT
$\text{HO}_2^+ + \text{H}_2\text{O}_2 \rightarrow \text{O}_2 + (\text{H}_2\text{O}_2)\text{H}^+$	-2.50		PT
D) Reactions of cations with H_2O		ΔH_r^0	
$\text{H}_2\text{O}_2^+ + \text{H}_2\text{O} \rightarrow \text{HO}_2 + \text{H}_3\text{O}^+$	-0.45		PT
$(\text{H}_2\text{O}_2)\text{H}^+ + \text{H}_2\text{O} \rightarrow \text{H}_2\text{O}_2 + \text{H}_3\text{O}^+$	-0.17		PT
$\text{H}_2\text{O}^+ + \text{H}_2\text{O} \rightarrow \text{OH} + \text{H}_3\text{O}^+$	-1.01		PT
$\text{OH}^+ + \text{H}_2\text{O} \rightarrow \text{O} + \text{H}_3\text{O}^+$	-2.14		PT
$\text{HO}_2^+ + \text{H}_2\text{O} \rightarrow \text{O}_2 + \text{H}_3\text{O}^+$	-2.67		PT
E) Complex reactions		ΔH_r^0	
$\text{H}_2\text{O}_2^+ + \text{H}_2\text{O}_2 \rightarrow \text{O}_2 + \text{OH} + \text{H}_3\text{O}^+$	-1.17		
$\text{H}_2\text{O}^+ + \text{H}_2\text{O}_2 \rightarrow \text{HO}_2 + \text{H}_3\text{O}^+$	-2.49		
$\text{OH}^+ + \text{H}_2\text{O}_2 \rightarrow \text{O}_2 + \text{H}_3\text{O}^+$	-5.82		

First part A) of Table 1 shows the dissociative ionization channels and the corresponding appearance energies AE according to NIST. At our ionization energy of 70 eV all these dissociative channels are opened. Therefore we consider further reactions of the corresponding radical species with the

most abundant compound in the clusters H_2O_2 in part B), and reactions of the nascent ions with H_2O_2 in part C). Part D) shows the ion reactions with H_2O molecules, which is the product of the radical (part B) and several cationic (part C) reactions, and it can also be present in the clusters as impurity. Some additional reactions are shown in part E), which are not necessarily elementary reactions but turned out energetically feasible.

Table 1 summarizes all reactions, which appear feasible, simply based on their exothermicity ($\Delta H_r^0 \leq 0$). This does not imply that all them take place in our clusters because of, e.g., kinetic and dynamics effects. However, it illustrates that the positive ion chemistry in our clusters can be very complex and complicated and there are quite a few reaction channels which could yield water molecules and hydronium H_3O^+ , besides water impurities in the clusters.

4 Pickup of pure O_2 on Ar_N clusters

4.1 Mass spectra

In the main article we argue that the major negative ion series $(\text{H}_2\text{O}_2)_n\text{O}_2^-$ does not originate from the thermal decomposition of H_2O_2 in the pickup cell and subsequent deposition of O_2 on Ar_M . Here, we present further evidence based on experiments with the pickup of pure O_2 on Ar_M clusters.

In the main article, there is no evidence for O_2 (nor O) containing series in the positive mass spectra. Is it possible that O_2 present in Ar_M cluster would be visible only in the negative ion spectrum but not exhibited in the positive one? To answer this question, we deposit pure O_2 directly on Ar_M . The clusters were generated under the same conditions as in the main article. Figure 3 shows the positive (top) and negative (bottom) ion mass spectra upon a higher oxygen pickup pressure of about 2.9×10^{-4} mbar. Under these pickup conditions, the mass peaks due to O_2 deposited on Ar_M start to be visible in the negative ion spectrum (bottom, red labeled). Clearly, strong O_2 containing series are observed in the positive spectrum (top) under the same conditions.

Figure 4 shows the mass spectra, when the oxygen pickup pressure is lowered to approximately 7×10^{-5} mbar. At this pressure, the O_2^- containing peaks in the negative spectrum (bottom) disappear completely. Nevertheless, clear O_2^+ containing peaks are still observable in the positive spectrum (top).

The mass peaks at $m/z = 79$ and 81 correspond to a trace contamination of our apparatus from previous experiments with HBr . We are looking for an evidence for very low signals here, thus we increase the sensitivity (detector voltage) as much as possible. This contamination normally does not appear in our spectra with any reasonable intensities under normal recording conditions. Similarly, the OH^- peak is due to the trace contamination of argon with water, discussed in the main article. It is much weaker than the corresponding mass peaks observed in the experiments with H_2O_2 . The O^- peak corresponds to the O_2 diffusion from the pickup cell into the mass spectrometer ionization region.

We can conclude from these experiments, that under the pickup conditions where there are enough O_2 molecules deposited on Ar_M , so that we can clearly observe various O and O_2 containing series in the positive spectra, we still could not detect any O_2^- (nor O^-) containing ions in the electron

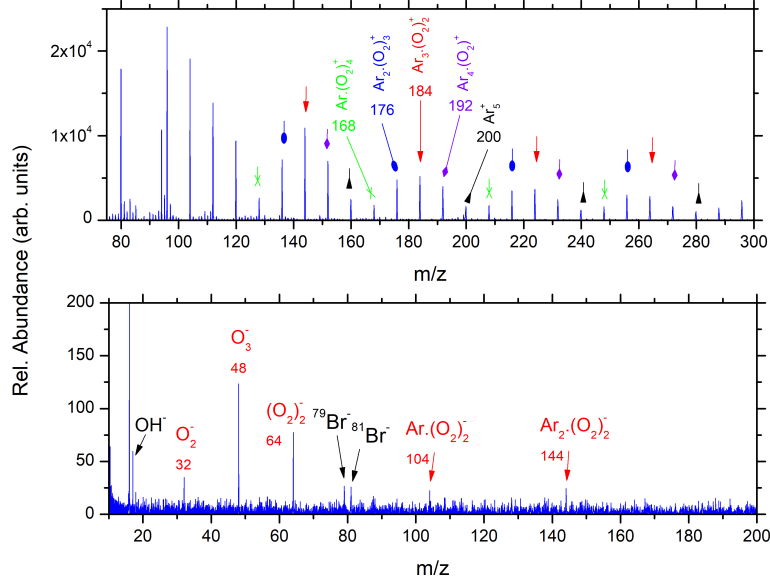


Figure 3. Positive (top) and negative (bottom) ion mass spectra of pure O_2 deposited directly on Ar_M clusters at higher concentrations ($P_{pickup} \approx 2.9 \times 10^{-4}$ mbar). The negative spectrum was integrated in the electron energy region 0-10 eV.

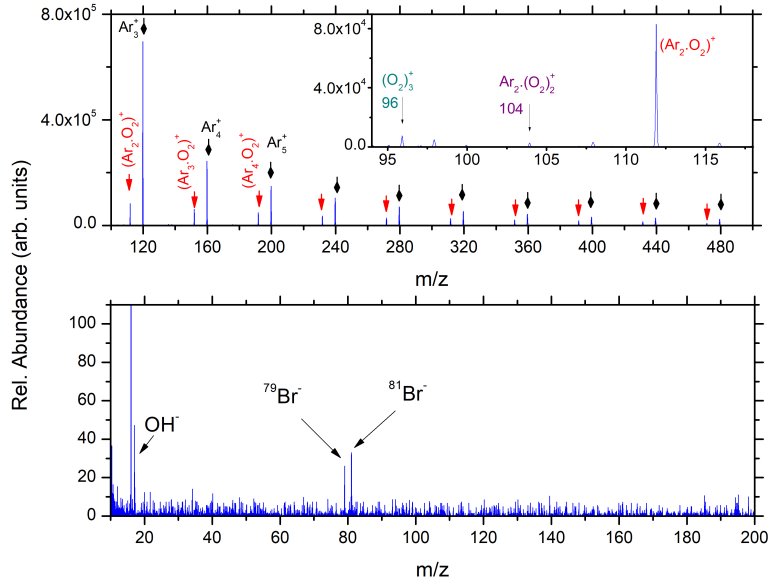


Figure 4. Positive (top) and negative (bottom) ion mass spectra of pure O_2 deposited directly on Ar_M clusters at low concentrations ($P_{pickup} \approx 7 \times 10^{-5}$ mbar). The negative spectrum was integrated in the electron energy region 0-10 eV. The major ion cluster series are labeled in the positive spectrum. The inset shows a detail of the spectrum where further observed series are shown. No oxygen containing clusters are observed in the negative ion mass spectrum.

attachment spectra (within our sensitivity limit $\approx 10^{-3}$ in the negative ion spectra). When we increase the O_2 amount in the pickup cell so that O_2^- containing ions are observable in the negative ion spectra, very strong oxygen containing cluster ion series are also present in the positive spectra. The detection limit in the positive ion spectra is about two orders of magnitude lower $\approx 10^{-5}$. Thus, in our experiments with hydrogen peroxide, the presence of oxygen containing series only in the negative ion spectra suggests that O_2 cannot be present in the clusters prior to the electron attachment.

4.2 Electron energy spectra

Figure 5 shows the electron energy spectra measured for O_2 deposited on Ar_M . Three spectra are shown for O^- (a), O_2^- (b), and $(O_2)_2^-$ (c). The major contribution to the O^- spectrum (a) is probably gas phase O_2 diffused from the pickup chamber to the ionization region (see above). Despite the low signal to noise, all the spectra exhibit unambiguous resonances at higher electron energies above 4 eV. This is in direct contradiction to the spectra from H_2O_2 on Ar_M in the main article, where there are no resonances above 4 eV. This again demonstrates that the negative ions observed in the H_2O_2 pickup stem from the electron attachment to H_2O_2 and not to O_2 on Ar_M .

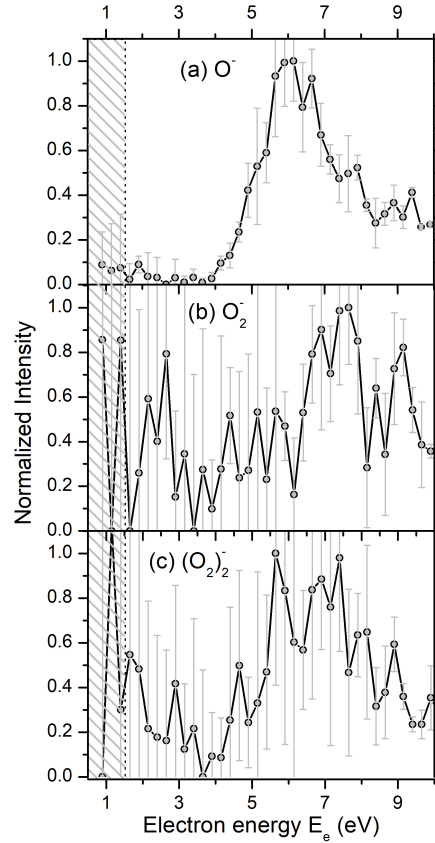


Figure 5. Electron energy spectra of (a) O^- , (b) O_2^- , (c) $(O_2)_2^-$ ions generated upon electron attachment to O_2 deposited on Ar_M clusters.